Electronic Supplementary Information (ESI)

Motional freedom of dimethylammonium ions in a cyanoelpasolite $[(CH_3)_2NH_2]_2KCo(CN)_6$ which exhibit phase transition associated with a distinct change of dielectric property

Tetsuo Asaji*

Department of Chemistry, College of Humanities and Sciences,

Nihon University, 3-25-40 Sakurajosui, Setagaya-ku, Tokyo 156-8550, Japan

E-mail: asaji@chs.nihon-u.ac.jp

Contents

References

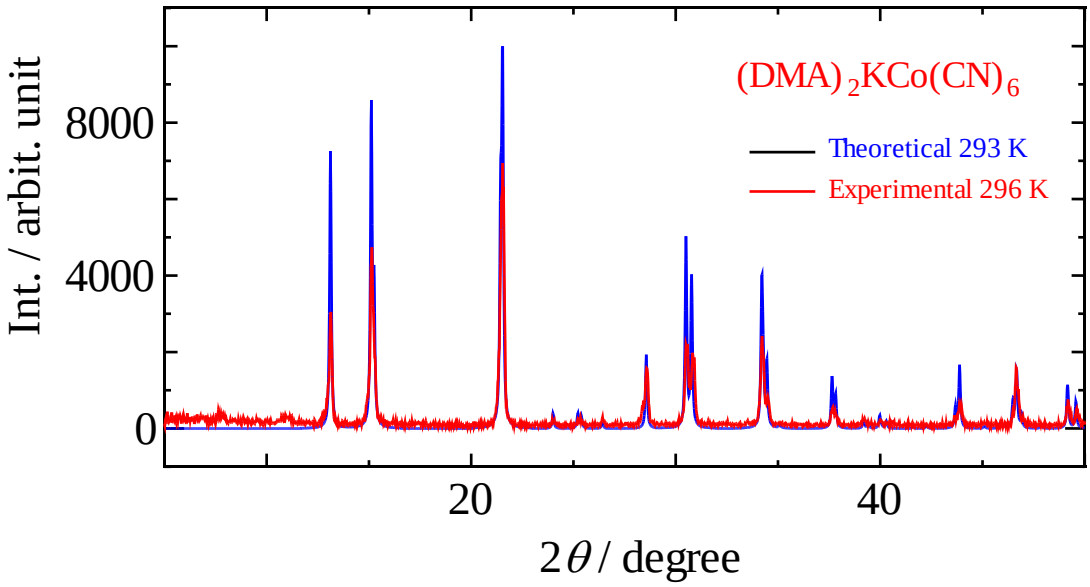

Fig. S1 Powder X-ray diffraction of $[(CH_3)_2NH_2]_2KCo(CN)_6$ by Cu Kα radiation. The abbreviation "DMA" stands for dimethylammonium. Theoretical pattern was calculated for *P4/mnc*, $a = b = 8.2895(13)$, $c = 11.621(3)$ Å, $Z = 2$ at 293 K [1]. The small peaks were observed at around 7.7 º and 11.0 º, which are close to the forbidden reflections (0 0 1) and (1 0 0) at 7.61 º and 10.67 º, respectively, calculated by the crystal data. This may indicate that the strict symmetry of the present crystals is lower than *P4/mnc*.

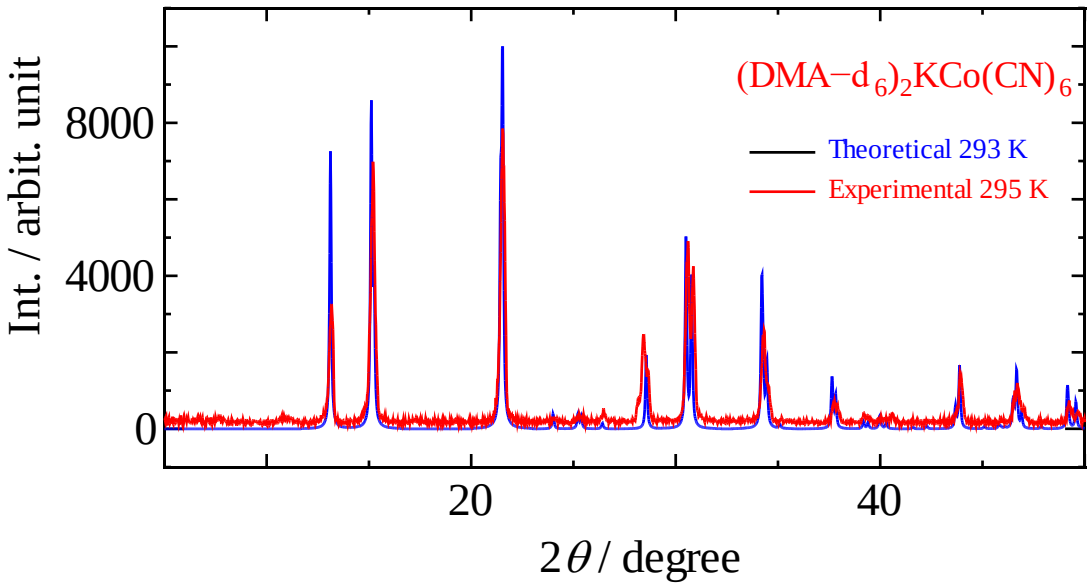

Fig. S2 Powder X-ray diffraction of $[(CD_3)_2NH_2]_2KCo(CN)_6$ by Cu Kα radiation. The abbreviation "DMA" stands for dimethylammonium. Theoretical pattern was calculated for *P4/mnc*, $a = b = 8.2895(13)$, $c = 11.621(3)$ Å, $Z = 2$ at 293 K [1]. The small peaks were observed at around 7.7 º and 10.9 º, which are close to the forbidden reflections (0 0 1) and (1 0 0) at 7.61 º and 10.67 º, respectively, calculated by the crystal data. This may indicate that the strict symmetry of the present crystals is lower than *P*4*/mnc*. There observed at room temperature no appreciable change of the crystal parameters by deuteration of the methyl groups.

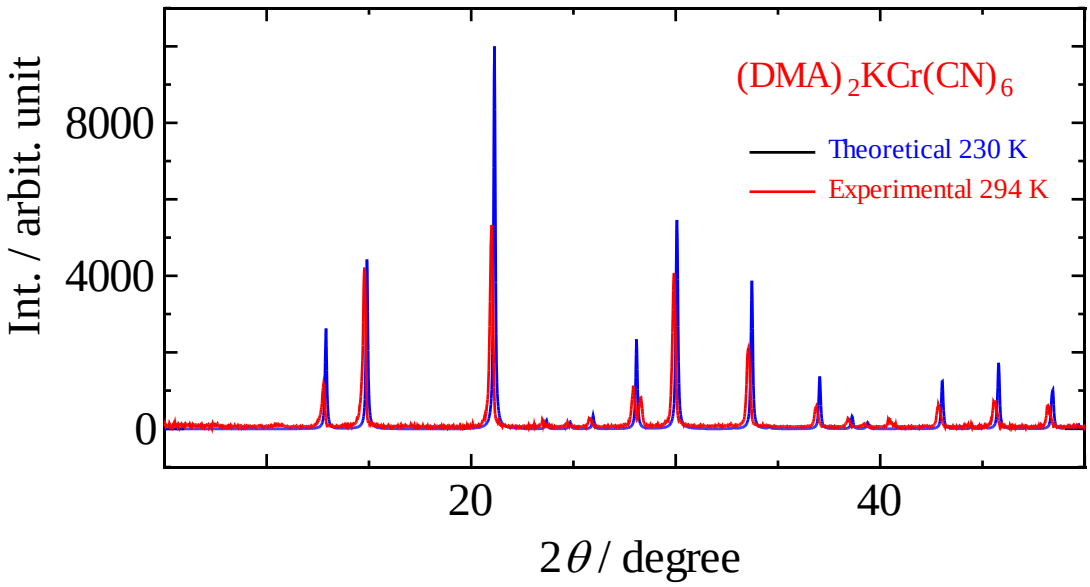

Fig. S3 Powder X-ray diffraction of $[(CH_3)_2NH_2]_2KCr(CN)_6$ by Cu Kα radiation. The abbreviation "DMA" stands for dimethylammonium. Theoretical pattern was calculated for *P4/mnc*, $a = b = 8.40300(10)$, $c = 11.8999(3)$ Å, $Z = 2$ at 230 K [2]. In the experimental pattern, the (2 0 0) and (2 2 0) reflections from KCl crystals can be recognized at 28.30 º and 40.44 º. Due to this contamination, the (2 1 2) reflection at 27.92 º of the title compound looks like to be split.

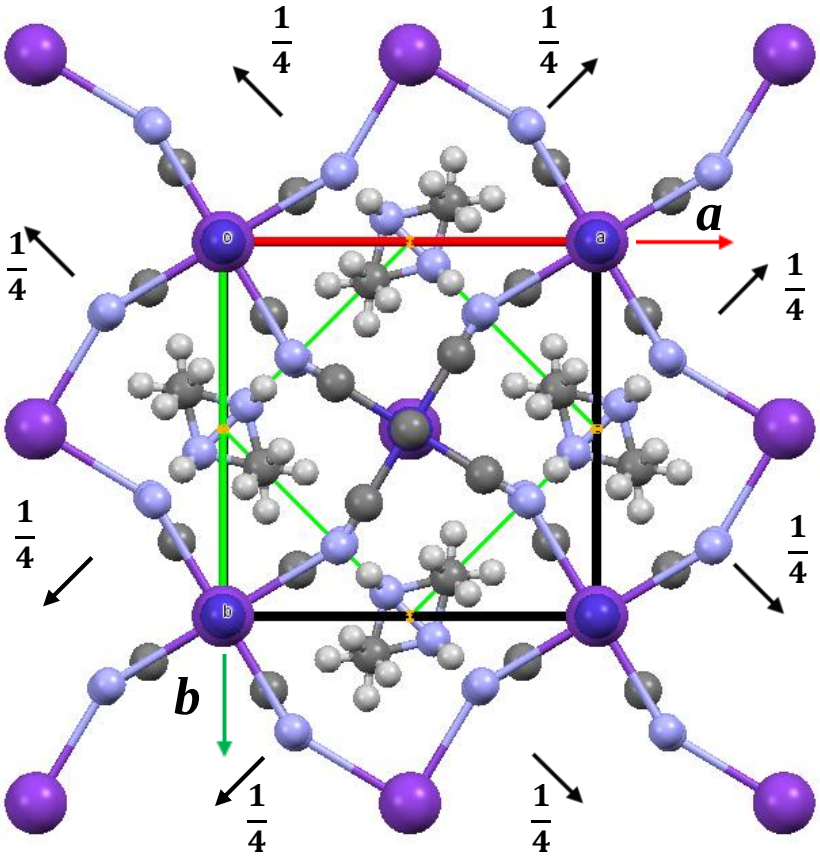

Fig. S4 Crystal structure of low-temperature phase of $[(CH_3)_2NH_2]_2KCo(CN)_6$ according to Zhang *et al* [1]. Space group *P*4/*mnc*, $a = b = 8.242(6)$, $c = 11.584(10)$ Å, $Z = 2$ at 113 K. Three two-fold rotation axes C_2 along [0 0 1], [1 1 0], and $[\bar{1}\,1\,0]$ directions go through the $(CH_3)_2NH_2^+$ ion site.

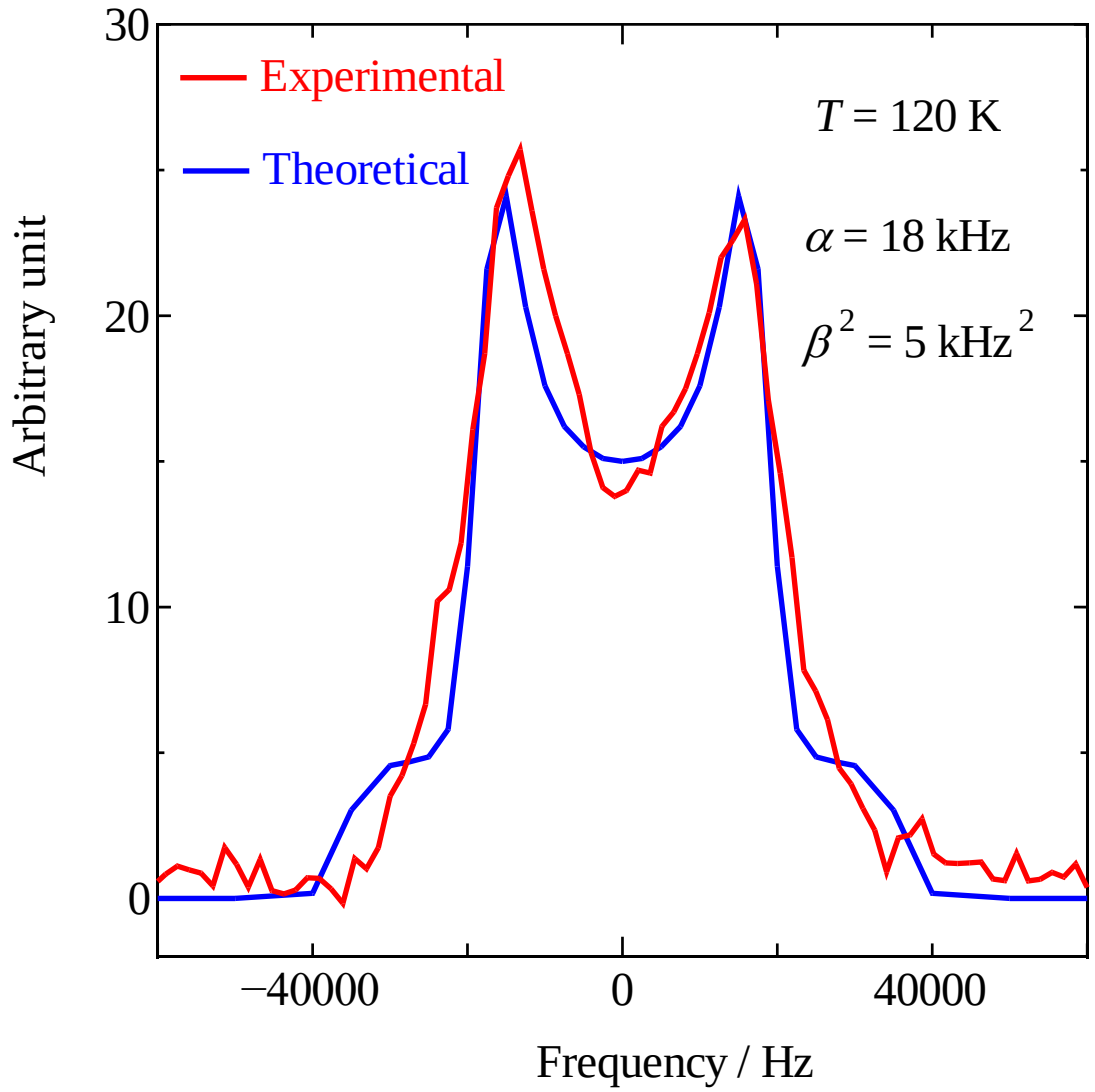

Fig. S5 ^{1}H NMR line of $[(CD_3)_2NH_2]_2KCo(CN)_6$ observed at 120 K (red line) and the simulated Pake doublet $F(x)$ (blue line). The argument x is the frequency deflection (Hz) from the center of the resonance. $F(x)$ is given by the following equations [3].

$$F(x) = N\int_{-\infty}^{+\infty} f(x')\exp\left(-\frac{(x-x')^2}{2\beta^2}\right)dx'$$

$$
\begin{aligned}
f(x) &= \left(-\frac{x}{\alpha}+1\right)^{-\frac{1}{2}} && -2\alpha \le x \le -\alpha \\
&= \left(-\frac{x}{\alpha}+1\right)^{-\frac{1}{2}} + \left(\frac{x}{\alpha}+1\right)^{-\frac{1}{2}} && -\alpha < x < \alpha \\
&= \left(\frac{x}{\alpha}+1\right)^{-\frac{1}{2}} && \alpha \le x \le 2\alpha
\end{aligned}
$$

where α is given as

$$\alpha = \frac{3\gamma^2\hbar}{8\pi r^3} \qquad (7)$$

by the proton-magnetogyric ratio γ and the distance r between the two protons, β represents line-broadening due to the dipolar interaction outside the pair protons, and N is a normalization factor.

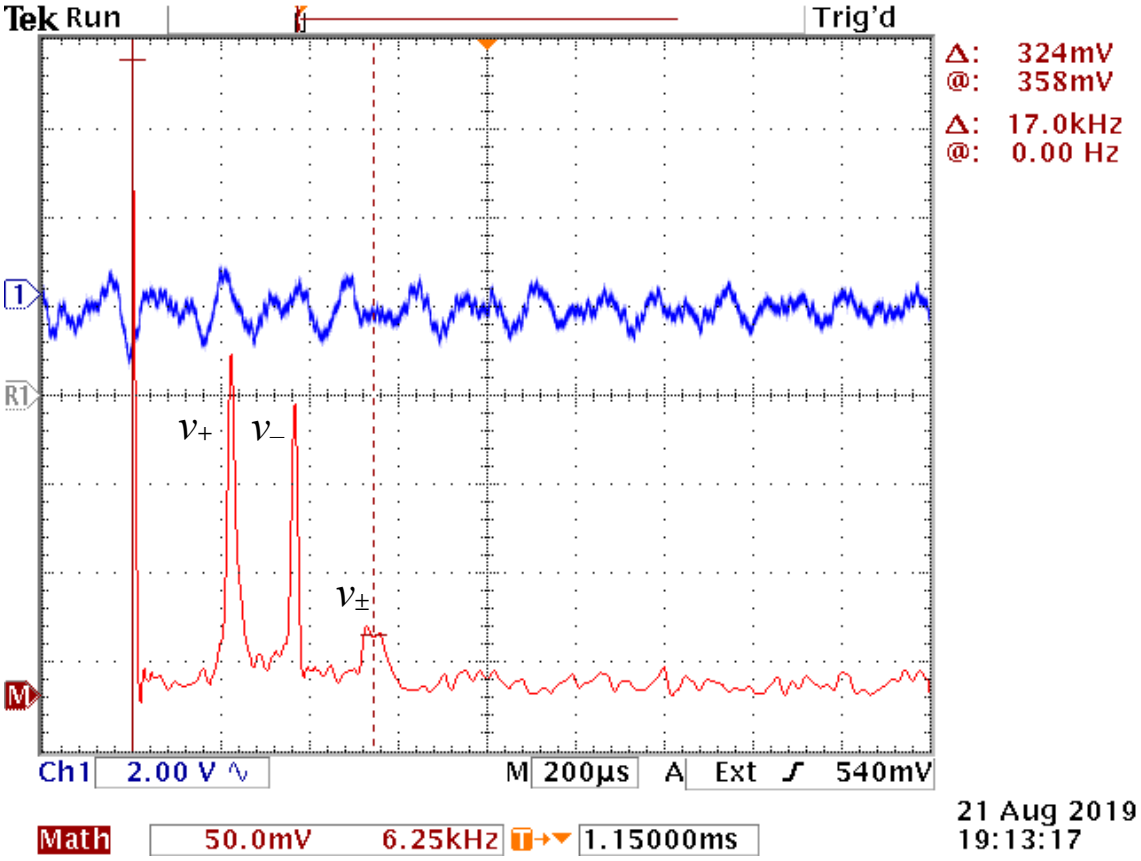

Fig. S6a ^{14}N NQR spectra of $(DMA)_2KCo(CN)_6$ at 298 K. Free induction decay (blue) and Fourier transform spectra (red) accumulated by 1024 times with the repetition time of 0.5 s. Since spectrometer frequency is 2618.0 kHz, ν_+ = 2625.0 kHz, ν_- = 2606.5 kHz, and $\nu_\pm$ = 2635.0 kHz.

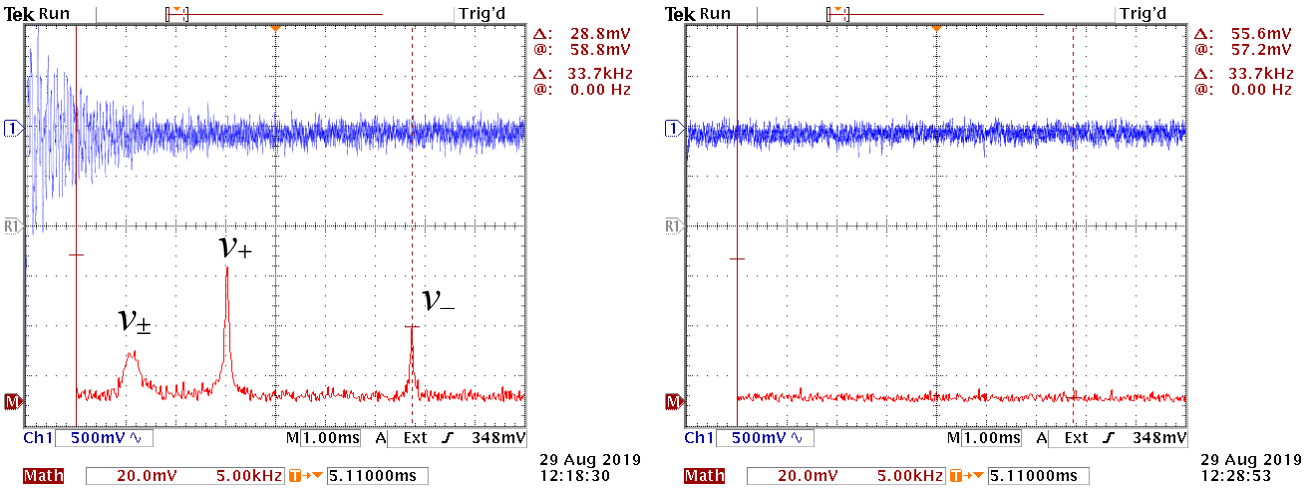

Fig. S6b Effect of magnetic field on ^{14}N NQR spectra of $(DMA)_2KCo(CN)_6$ at 297.5 K. Spectrometer frequency RF = 2640.0 kHz, number of accumulation N = 2048, repetition time t = 0.2 s. With (right) and without (left) magnetic field of *ca*. 110 G.

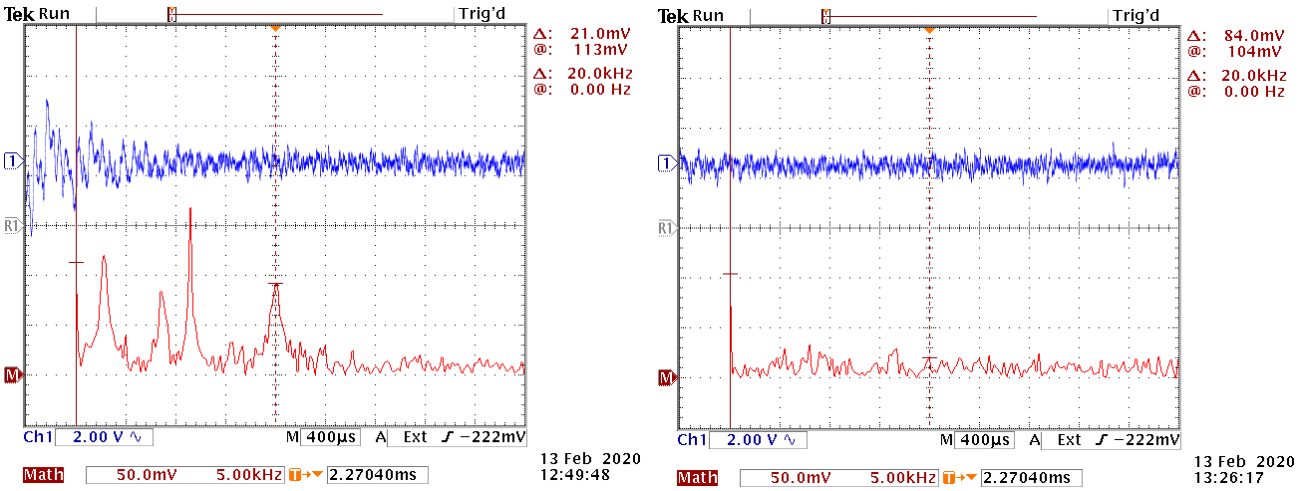

Fig. S6c Effect of magnetic field on ^{14}N NQR spectra of $(DMA)_2KCo(CN)_6$ at 77.3 K. Spectrometer frequency RF = 2680.0 kHz, number of accumulation N = 256, repetition time t = 5 s. With (right) and without (left) magnetic field of *ca*. 110 G.

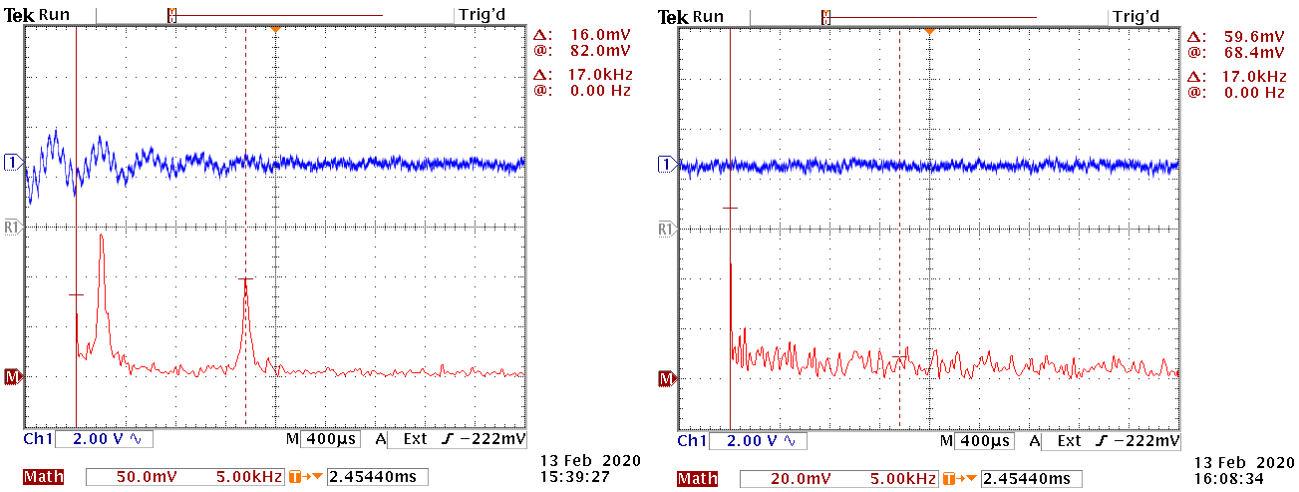

Fig. S6d Effect of magnetic field on ^{14}N NQR spectra of $(DMA)_2KCo(CN)_6$ at 77.3 K. Spectrometer frequency RF = 2740.0 kHz, number of accumulation *N* = 1024, repetition time *t* = 1 s. With (right) and without (left) magnetic field of *ca*. 110 G.

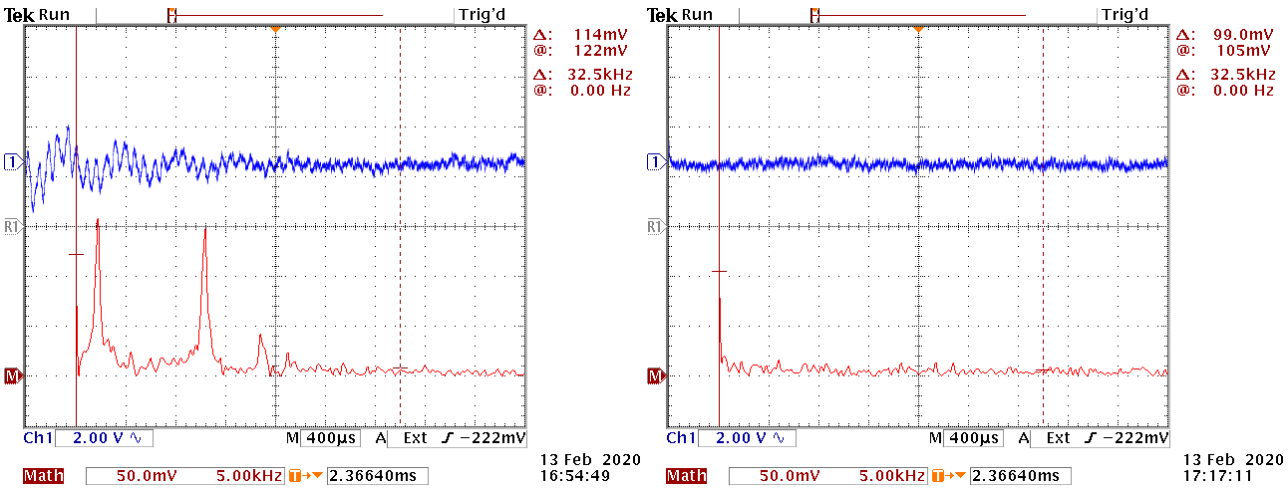

Fig. S6e Effect of magnetic field on ^{14}N NQR spectra of $(DMA)_2KCo(CN)_6$ at 77.3 K. Spectrometer frequency RF = 2710.0 kHz, number of accumulation *N* = 1024, repetition time *t* = 1 s. With (right) and without (left) magnetic field of *ca*. 110 G.

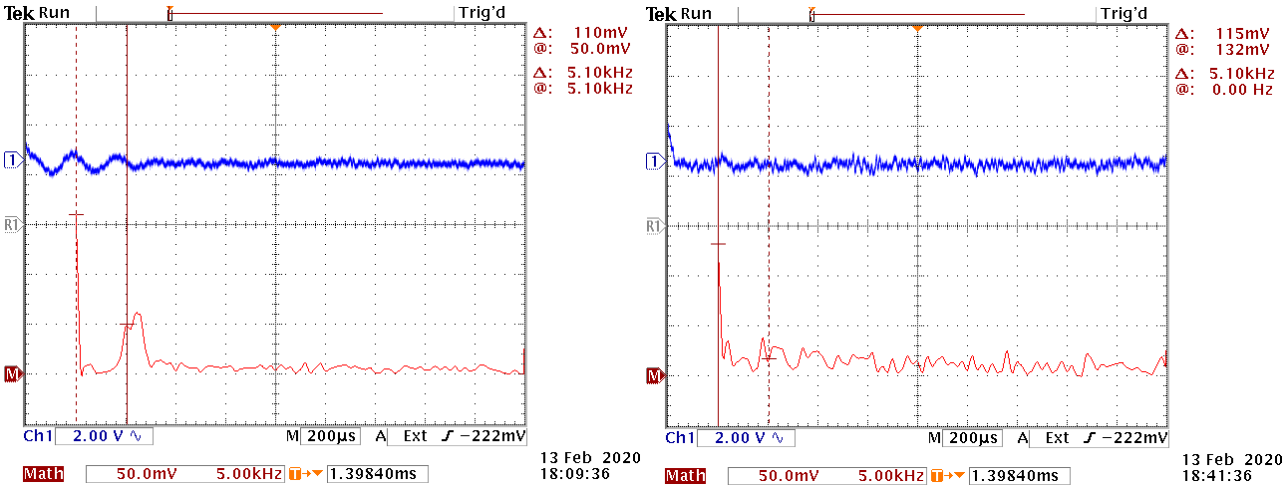

Fig. S6f Effect of magnetic field on ^{14}N NQR spectra of $(DMA)_2KCo(CN)_6$ at 77.3 K. Spectrometer frequency RF = 2774.0 kHz, number of accumulation N = 512, repetition time t = 3 s. With (right) and without (left) magnetic field of *ca*. 110 G.

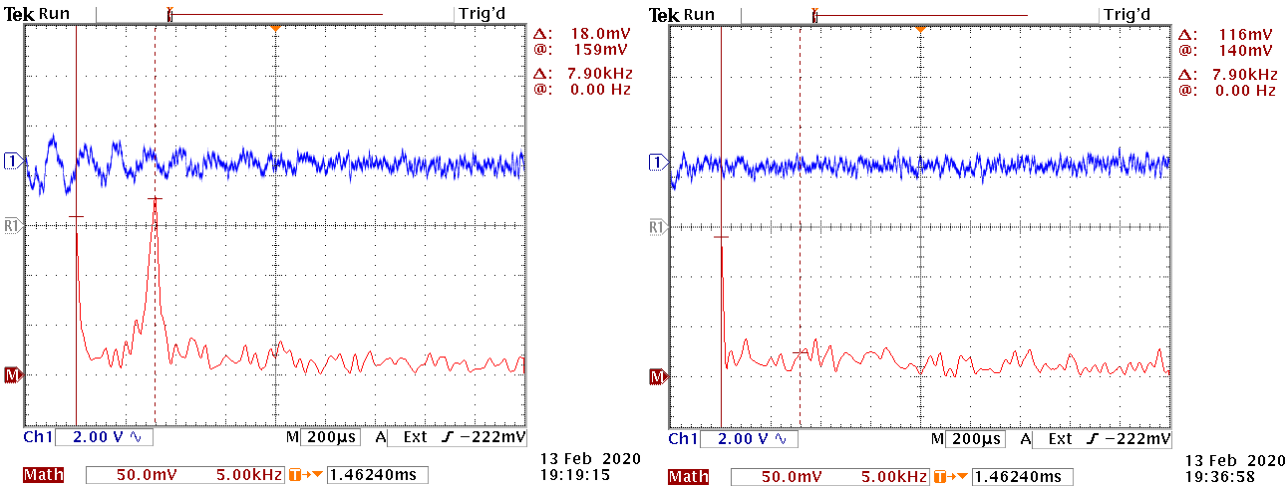

Fig. S6g Effect of magnetic field on ^{14}N NQR spectra of $(DMA)_2KCo(CN)_6$ at 77.3 K. Spectrometer frequency RF = 2600.0 kHz, number of accumulation N = 256, repetition time t = 3 s. With (right) and without (left) magnetic field of *ca*. 110 G.

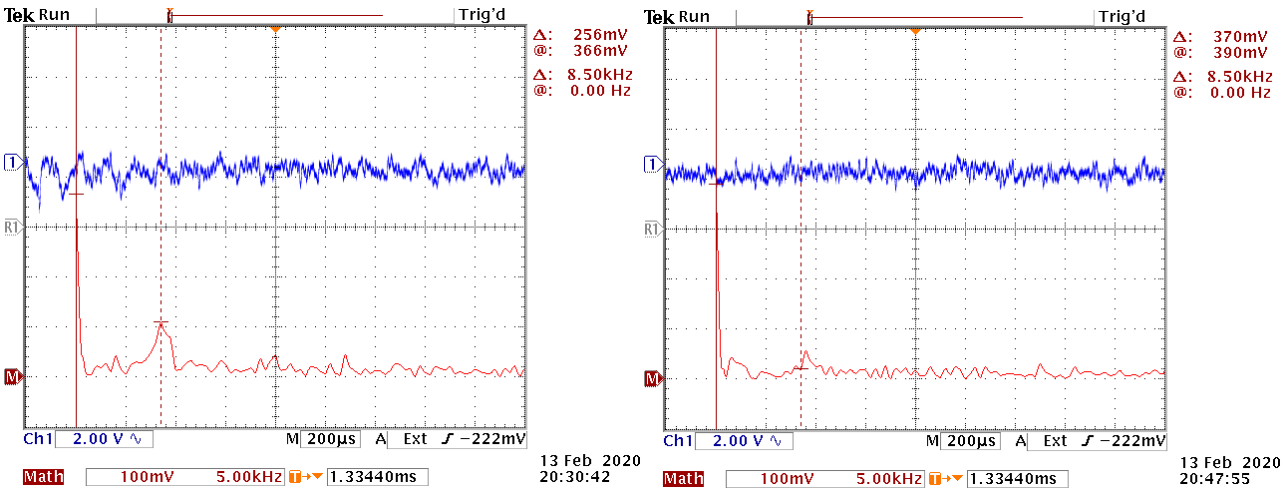

Fig. S6h Effect of magnetic field on ^{14}N NQR spectra of $(DMA)_2KCo(CN)_6$ at 77.3 K. Spectrometer frequency RF = 2640.0 kHz, number of accumulation N = 256, repetition time t = 3 s. With (right) and without (left) magnetic field of *ca*. 110 G.

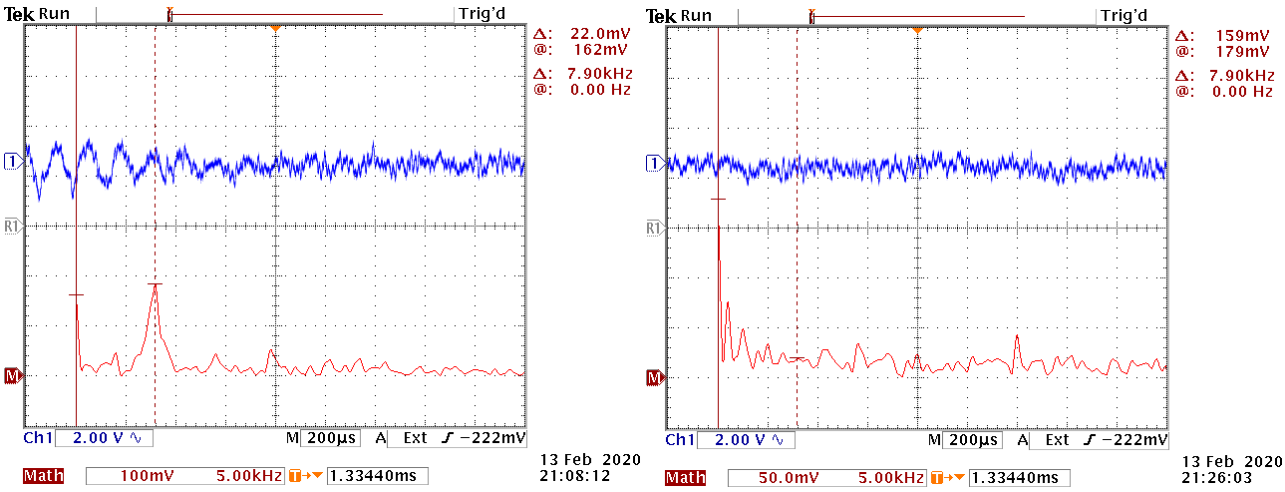

Fig. S6i Effect of magnetic field on ^{14}N NQR spectra of $(DMA)_2KCo(CN)_6$ at 77.3 K. Spectrometer frequency RF = 2580.0 kHz, number of accumulation N = 256, repetition time t = 3 s. With (right) and without (left) magnetic field of *ca*. 110 G.

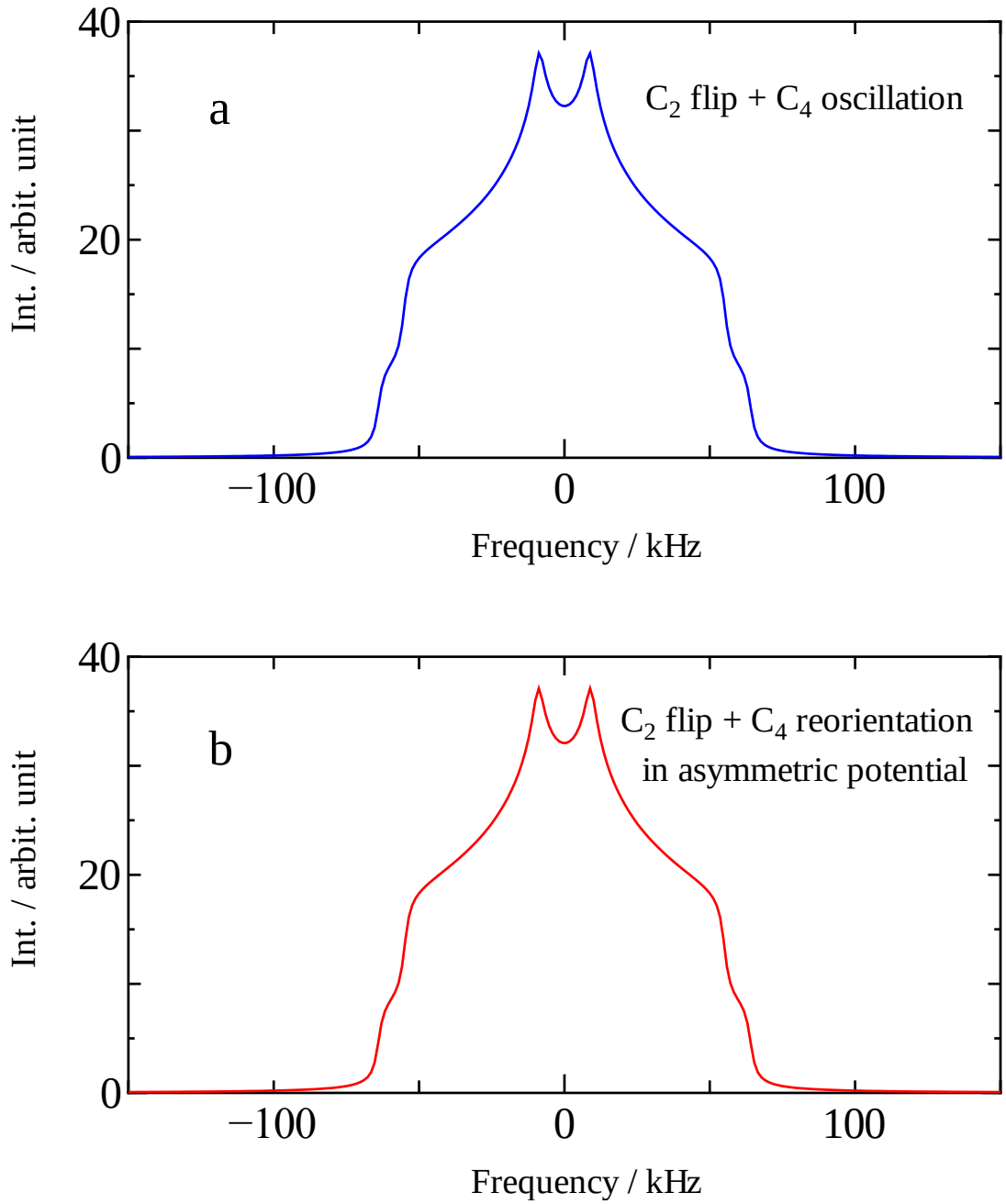

Fig. S7 ^{2}H NMR spectra simulation. The D-N-D bond angle was set at 107°. The quadrupole coupling constant of 128 kHz and the asymmetry parameter η = 0 were used. The calculation was done by use of "NMR Weblab, A Tool for Simulation of Solid State NMR Spectra 6.6.2" [4]. As for the axis notation, see Fig. 7 in the text. (a) ^{2}H NMR line-shape calculated assuming very fast C_2 flip about the $C_{2,\eta}$ axis and fast rotational oscillation about the $C_{2,\zeta}$ axis (pseudo C_4 axis) with Gaussian jump angle distribution full width of 35°. (b) ^{2}H NMR line-shape calculated assuming very fast C_2 flip about the $C_{2,\eta}$ axis and fast four sites reorientation among A, B, A', B' sites with population of 0.91 at A or A' and 0.09 at B or B' (pseudo C_4 reorientation about the $C_{2,\zeta}$ axis).

References

[1] W. Zhang, H.-Y. Ye, R. Graf, H. W. Spiess, Y.-F. Yao, R.-Q. Zhu, and R.-G. Xiong, *J. Am. Chem. Soc.,* 2013, **135**, 5230-5233.

[2] M. Rok, G. Bator, B. Zarychta, B. Dziuk, J. Repeć, W. Medycki, M. Zamponi, G. Usevičius, M. Šimėnas, and J. Banys, *Dalton Trans.*, 2019, **48**, 4190-4202.

[3] T. Asaji and K. Ashitomi, *J. Phys. Chem. C*, 2013, **117**, 10185-10190; A. Abragam, *The Principles of Nuclear Magnetism*, Oxford University Press, London, 1961.

[4] V. Macho, L. Brombacher, and H. W. Spiess, *Appl. Magn. Reson.* 2001, **20**, 405-432.